Inorganica Chimica Acta 363 (2010) 2886–2895

Contents lists available at ScienceDirect

Inorganica Chimica Acta

journal homepage: www.elsevier.com/locate/ica

Anion binding studies of tris(2-aminoethyl)amine based amide receptors with nitro functionalized aryl substitutions: A positional isomeric effect

I. Ravikumar, P.S. Lakshminarayanan, Pradyut Ghosh *

Department of Inorganic Chemistry, Indian Association for the Cultivation of Science, 2A&2B Raja S.C. Mullick Road, Kolkata 700032, India

ARTICLE INFO

Article history:
Received 14 January 2010
Accepted 22 February 2010
Available online 25 February 2010

Dedicated to Animesh Chakravorty

Keywords:
Anion recognition
Neutral receptor
Amide
Hydrogen bonds
X-ray crystallography
Supramolecular chemistry

ABSTRACT

Syntheses and crystal structures of tren-based amide, $\mathbf{L^1}$, *N*,*N*′,*N*″-tris[(2-amino-ethyl)-4-nitro-benzamide] and $\mathbf{L^2}$, *N*,*N*′,*N*″-tris[(2-amino-ethyl)-2-nitro-benzamide] are reported and compared with previously published tripodal amide receptor $\mathbf{L^3}$, *N*,*N*′,*N*″-tris[(2-amino-ethyl)-3-nitro-benzamide]. The crystallographic results show intramolecular and intermolecular hydrogen-bonding interactions between two arms of the tripodal receptor and two other adjacent molecules in cases of $\mathbf{L^1}$ and $\mathbf{L^2}$ whereas in addition to the above interactions an aromatic π···π stacking among tripodal arms is also observed in $\mathbf{L^3}$. Receptors $\mathbf{L^1}$, $\mathbf{L^2}$ and $\mathbf{L^3}$ having electron withdrawing $-NO_2$ substituted (*para, ortho* and *meta*, respectively) phenyl moieties are explored toward their solution state anion binding properties and selectivity studies. The substantial changes in chemical shifts are observed for the amide protons (–N*H*) and aromatic protons (–C*H*) with F^- and Cl^- in cases of $\mathbf{L^1}$ and $\mathbf{L^3}$, and only with F^- for $\mathbf{L^2}$, indicating the participation of –NH and –CH protons in the solution state binding events. Binding constants for the above cases are calculated by ^{1}H NMR titration upon monitoring the –NH signal. Receptor $\mathbf{L^2}$ shows exclusive selectivity toward F^- in dimethyl sulfoxide (DMSO). The structural aspects of binding I^-, ClO_4^- and SiF_6^{2-} with the monoprotonated $\mathbf{L^1}$, $\mathbf{L^1}H^+{\cdot}I^-{\cdot}$DMF (**1**), $\mathbf{L^1}H^+{\cdot}ClO_4^-{\cdot}$DMF (**2**) and $\mathbf{L^1}H^+{\cdot}0.5SiF_6^{2-}{\cdot}H_2O$ (**3**), respectively are examined crystallographically. Anion binding with multiple receptor units is observed *via* amide N–H···anion as well as aryl C–H···anion hydrogen-bonding interactions in all the complexes as observed in cases of previously reported crystal structures of anionic complexes of protonated $\mathbf{L^3}$. The aryl group having nitro functionality that contributes to solution state anion binding with the neutral receptor and solid state coordination in complexes **1**–**3** through CH···anion interactions is noteworthy.

1. Introduction and background

The design and syntheses of receptors capable of binding anionic guests is of crucial importance due to their potential applications in environmental, biological processes and molecular recognition studies [1–20]. In 1993 Reinhoudt and co-workers introduced a series of tris(2-aminoethyl)-amine, tren-based tripodal ligands containing amide or sulfonamide groups as anion receptors, where a conductivity study showed binding preference in the order $H_2PO_4^- > Cl^- > HSO_4^-$ [21]. Later tren has been studied as an important building block in tripodal receptor systems having amine, amide and urea functionality for anions by us [28,35–37], and different groups [21–27,29–34]. Anion receptors in nature often involve amide linkages as hydrogen-bond donors; hence, amide based receptors are important for anion binding study [1–9,21]. Beer et al. have shown halide and ReO_4^- binding in the tripodal amide by ^{1}H NMR titration studies [22]. These early reports of anion binding with tren-based tripodal amide receptors in solution by Reinhoudt and Beer are explained by hydrogen-bond formation between the amide functionality of receptor and the anion. Structural information can provide insight on the proper binding topology of anions with these tripodal amide receptors. In this regard, Bowman-James et al. showed that the nitrate salt of a monoprotonated tripodal lipophilic amide receptor, where anion is not encapsulated in the cavity of a tren unit. This is simply because one of the amide carbonyl oxygen atom points into the cavity to hydrogen-bond with the *endo* oriented part of the apical amine as observed from the structural investigation [25]. Theoretical investigation by Hay et al. showed that the effect of electron withdrawing substituents on the aryl moiety significantly enhances the stability of anion complexes [33]. The binding ability of tren-based acyclic tripodal receptors toward anions varies with the attached moiety to the tren (N4) unit, since functional groups modify the hydrogen bonding capability [33], as well as the conformation of the receptor [35–37]. We have reported the coordination of a monoprotonated tren-based triamide, $\mathbf{L^3}$, having nitro functionality at the *meta* position with anionic guests of different shapes and geometry [28]. Given our interest in both solution and structural aspects of anion binding, herein, we report three tren-based tripodal amide

* Corresponding author. Tel.: +91 33 2473 4971; fax: +91 33 2473 2805.
E-mail address: icpg@iacs.res.in (P. Ghosh).

0020-1693/$ - see front matter © 2010 Elsevier B.V. All rights reserved.
doi:10.1016/j.ica.2010.02.030

receptors $\mathbf{L^1}$–$\mathbf{L^3}$ (see Chart 1) and their solution state anion binding studies in neutral form *via* detailed ^{1}H NMR studies along with structures of $\mathbf{L^1}$, $\mathbf{L^2}$, and binding of I^- (spherical), **1**, ClO_4^- (tetrahedral), **2**, and SiF_6^{2-} (octahedral), **3**, with $[H\mathbf{L^1}]^+$ and their detailed molecular interactions. We also demonstrate the effect of positional isomers toward the selective binding of F^- with $\mathbf{L^2}$ in solution.

2. Experimental section

2.1. Materials

Tris(2-aminoethyl) amine, 2-nitrobenzoyl chloride, 3-nitrobenzoyl chloride, and 4-nitrobenzoyl chloride and tetrabutylammonium salts of fluoride, chloride, bromide, iodide, dihydrogenphosphate, hydrogensulfate, perchlorate and nitrate were purchased from Aldrich chemicals and used as received. Hydroiodic acid, and perchloric acid were received from SD Fine Chemicals, India, and hydrofluoric acid was received from Merck, India. All the solvents and triethylamine were purchased from SD Fine Chemicals, India, and were purified prior to use.

2.2. Syntheses

The tripodal amide receptors $\mathbf{L^1}$–$\mathbf{L^3}$ were synthesized following our literature procedure [28]. A representative synthesis of $\mathbf{L^1}$ is presented here. Reaction of tren with 4-nitrobenzoyl chloride in a 1:3 molar ratio at room temperature yielded $\mathbf{L^1}$ in high yield. 0.146 g, 1 mmol of tren, was dissolved in 30 mL of dry tetrahydrofuran (THF) in a 150 mL two neck round bottomed flask. 0.354 g (3.5 mmol) of dry triethylamine (Et_3N) was added to the reaction mixture and stirred at room temperature under nitrogen atmosphere for 30 min. A solution of 4-nitrobenzoyl chloride (0.557 g, 3 mmol) in 50 mL of dry THF was added drop-wise to the reaction mixture over a period of 1 h under nitrogen atmosphere with constant stirring at room temperature. After the addition was completed, a pale yellow precipitate is formed and the reaction mixture was allowed to stir at room temperature for overnight. The light yellow precipitate formed was filtered through a filter paper and washed three times with (3 × 100 mL) of water, two times with (2 × 10) mL of cold THF and dried in air. The yellow solid was re-dissolved in DMF and allowed to evaporate slowly at room temperature. Single crystals of $\mathbf{L^1}$ suitable for X-ray diffraction studies were obtained after two days in 95% yield. Complexes **1**, **2**, and **3** were obtained by dissolving $\mathbf{L^1}$ (50 mg) in 50 mL of DMF and adding 1.5 equiv of 37% HI, 70% $HClO_4$, and 40% HF, respectively. The respective solutions were stirred at room temperature for 30 min and filtered in a 100 mL beaker. Filtrates were allowed to evaporate at room temperature, which yielded suitable crystals for X-ray analysis in 4 days. Single crystals of $\mathbf{L^2}$ were also obtained from DMF.

2.2.1. $\mathbf{L^1}$

Yield: 95%, ^{1}H NMR (300 MHz, DMSO-d_6): δ 3.31 (m, 6H, NCH_2CH_2), 3.83 (m, 6H, NCH_2CH_2), 7.95 (d, 6H, Ar*H*, J = 7.0 Hz), 8.16 (d, 6H, Ar*H*, J = 7. 0 Hz), 8.78 (br, 3H, −NH). ^{13}C NMR (75 MHz, DMSO-d_6): δ 43.40 (NCH_2), 53.55 (NCH_2CH_2), 127.99, 135.03, 140.03, and 151.68 (Ar), 168.94 (C═O). HRMS (ESI): m/z 594.2132 $[\mathbf{L^1}]^+$.

2.2.2. $\mathbf{L^2}$

Yield: 95%, ^{1}H NMR (300 MHz, DMSO-d_6): δ 2.72 (t, 6H, NCH_2CH_2), 3.39 (t, 6H, NCH_2CH_2), 7.55 (d, 3H, Ar*H*), 7.57 (m, 6H, Ar*H*), 7.99 (d, 3H, Ar*H*), 8.60 (t, 3H, −N*H*). ^{13}C NMR (75 MHz, DMSO-d_6): δ 45.40 (NCH_2), 56.20 (NCH_2CH_2), 126.79, 128.41, 130.22, 134.88, 136.41, and 148.72 (Ar), 167.65 (C═O). HRMS (ESI): m/z 594.3674 $[\mathbf{L^2}]^+$.

2.2.3. $\mathbf{L^1}H^+I^-\cdot DMF$, **1**

Yield: 75%, ^{1}H NMR (300 MHz, DMSO-d_6): δ 3.26 (m, 6H, NCH_2CH_2), 3.71 (m, 6H, NCH_2CH_2), 8.10 (d, 6H, Ar*H*, J = 7. 0 Hz), 8.18 (d, 6H, Ar*H*, J = 7. 0 Hz), 8.72 (br, 3H, –NH). ^{13}C NMR (75 MHz, DMSO-d_6): δ 43.44 (NCH_2), 53.14 (NCH_2CH_2), 128.02, 134.98, 139.68, and 152.09 (Ar), 169.14 (C═O).

2.2.4. $\mathbf{L^1}H^+ClO_4^-\cdot DMF$, **2**

Yield: 60%, ^{1}H NMR (300 MHz, DMSO-d_6): δ 3.33 (m, 6H, NCH_2CH_2), 3.71 (m, 6H, NCH_2CH_2), 8.00 (d, 6H, Ar*H*, J = 7. 0 Hz), 8.21 (d, 6H, Ar*H*, J = 7. 0 Hz), 8.79 (br, 3H, -NH). ^{13}C NMR (75 MHz, DMSO-d_6): δ 42.92 (NCH_2), 53.89 (NCH_2CH_2), 126.98, 134.99, 140.12, and 152.03 (Ar), 168.94 (C═O).

2.2.5. $\mathbf{L^1}H^+0.5SiF_6^{2-}\cdot H_2O$, **3**

Yield: 55%, ^{1}H NMR (300 MHz, DMSO-d_6): δ 3.31 (m, 6H, NCH_2CH_2), 3.71 (m, 6H, NCH_2CH_2), 7.98 (d, 6H, Ar*H*, J = 7. 0 Hz), 8.22 (d, 6H, Ar*H*, J = 7.0 Hz), 8.78 (br, 3H, –NH). ^{13}C NMR (75 MHz, DMSO-d_6): δ 42.69 (NCH_2), 53.57 (NCH_2CH_2), 126.87, 134.87, 139.99, and 150.98 (Ar), 168.94 (C═O).

3. Methods

^{1}H and ^{13}C NMR spectra were recorded on a Bruker 300 MHz and a 75 MHz FT-NMR spectrometer (model: Avance-DPX300), respectively. HRMS (+ESI) measurements were carried out on Waters QTof-Micro instruments.

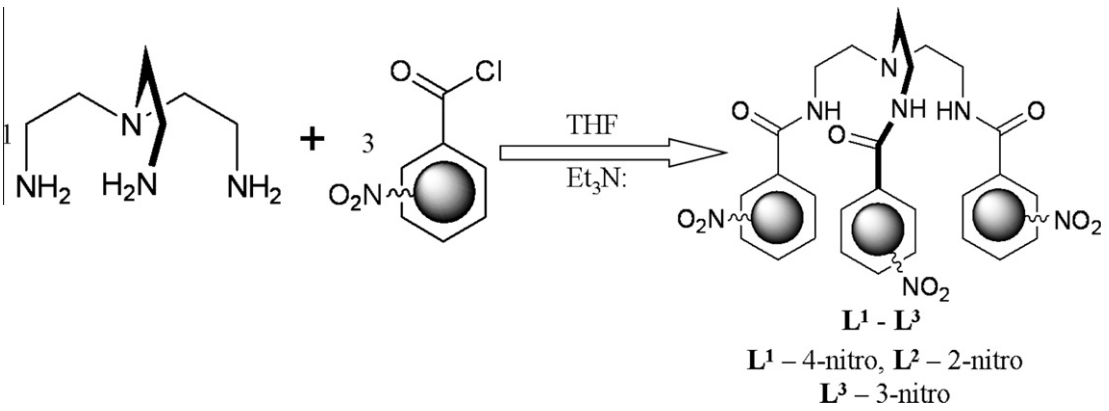

Chart 1. General synthesis of $\mathbf{L^1}$–$\mathbf{L^3}$.

3.1. ^{1}H NMR titration experiments

Binding constants were obtained by ^{1}H NMR (300 MHz Bruker) titrations of $\mathbf{L^1}$–$\mathbf{L^3}$ with tetrabutylammonium salts of respective halides in DMSO-d_6 at 25 °C. The initial concentration of corresponding receptor was 20 mM. Aliquots of anions were added from two different stock solutions 25 mM and 50 mM of anions (host: guest = up to 1:1, 25 mM stock solution was used, and above 1:1 ratio higher concentration anion was used). Tetramethylsilane (TMS) in DMSO-d_6 was used as an internal reference, and each titration was performed by 15 measurements at room temperature. All the proton signals were referred to TMS. The association constants, $\boldsymbol{K}$, were calculated by fitting the change in the N–H chemical shift with a 1:1 association model with non-linear least square analysis. WINEQNMR 2.0 was employed in the calculation of association constants [38]. The error limit in $\boldsymbol{K}$ was less than 10%.

Following equation was used to determine the $\boldsymbol{K}$ values.

$$\Delta\delta = \{([A]_0 + [\mathbf{L}]_0 + 1/\mathbf{K}) \pm (([A]_0 + [\mathbf{L}]_0 + 1/\mathbf{L})^2 - 4[\mathbf{L}]_0[A]_0)^{1/2}\}\Delta\delta_{max}/2[\mathbf{L}]_0$$

3.2. X-ray crystallography

The crystallographic data and details of data collection for $\mathbf{L^1}$, $\mathbf{L^2}$ and salts **1**–**3** are given in Table 1. In each case, a crystal of suitable size was selected from the mother liquor and immersed in partone oil, and then it was mounted on the tip of a glass fiber and cemented using epoxy resin. Intensity data for all crystals were collected using Mo Kα (0.71073 Å) radiation on a Bruker SMART APEX diffractometer equipped with a CCD area detector at 100 K ($\mathbf{L^1}$, $\mathbf{L^2}$, **1** and **2**) and at 273 K for complex **3**. The data integration and reduction were processed with SAINT [39] software. An empirical absorption correction was applied to the collected reflections with SADABS [40] using XPREP [39]. The structures were solved by direct methods using SHELXTL [41] and were refined on F^2 by the full-matrix least-squares technique using the SHELXL-97 [42] program package. Graphics were generated using PLATON [43] and MERCURY 2.3 [44]. In all five compounds, non-hydrogen atoms were refined anisotropically. Hydrogen atoms attached to all carbon atoms were geometrically fixed while the hydrogen atoms of amide, tertiary amino nitrogen of the salts, were located from the difference Fourier map, and the positional and temperature factors were refined isotropically. In complex **3**, the hydrogen atoms attached to lattice water molecule could be located from difference Fourier map.

4. Results and discussion

4.1. Syntheses

Acyclic tripodal receptors $\mathbf{L^1}$–$\mathbf{L^3}$ have been synthesized in high yield, and the single-crystal X-ray studies are performed to understand the binding capacity of $\mathbf{L^1}$ with different anions in monoprotonated state. Syntheses of $\mathbf{L^1}$–$\mathbf{L^3}$ are straightforward and involve a simple addition of respective acid chlorides to the solution of tren in presence of Et_3N. Single crystals of $\mathbf{L^1}$ and $\mathbf{L^2}$ suitable for X-ray studies are obtained by slow evaporation of DMF solution in high yield. Complexes **1**–**3** are obtained by titrating $\mathbf{L^1}$ with respective acids in DMF solvent, and crystallization is obtained by slow evaporation. Syntheses of these salts are also straightforward, resulting in high yields. Isolation of any salt of $\mathbf{L^2}$ was unsuccessful in this experimental conditions.

4.2. Solution studies

The host-guest chemistry between receptors and anions in solution is immediately detected by a dramatic increase in the solubility of the receptor in nonpolar solvents like CH_2Cl_2, $CHCl_3$, and $CH_3COOC_2H_5$ upon the addition of tetrabutylammonium fluoride/chloride whereas $\mathbf{L^1}$–$\mathbf{L^3}$ have solubility only in polar solvents like DMSO or DMF. To study the positional isomeric effect, we have synthesized $\mathbf{L^1}$, $\mathbf{L^2}$ and $\mathbf{L^3}$ where nitro group is placed at the *para*, *ortho* and *meta* positions, respectively with respect to the amide group of receptors. Solution binding properties of these receptors with different halides, oxyanions are investigated by ^{1}H-NMR experiments in DMSO-d_6 at 25 °C. Based on the effect of positional isomers toward anion selectivity we describe the solution state binding data in following order i.e $\mathbf{L^3}$, followed by $\mathbf{L^1}$ and $\mathbf{L^2}$. The

Table 1
Crystal data and structure refinement for $\mathbf{L^1}$, $\mathbf{L^2}$, complexes [H$\mathbf{L^1}$]·I·DMF (**1**), [H$\mathbf{L^1}$]·ClO_4·DMF (**2**) and [H$\mathbf{L^1}$]·0.5SiF_6·H_2O (**3**).

	$\mathbf{L^1}$	$\mathbf{L^2}$	**1**	**2**	**3**
CCDC number	760009	760008	760005	760006	760007
Empirical formula	$C_{54}H_{54}N_{14}O_{18}$	$C_{27}H_{27}N_7O_9$	$C_{36}H_{20}IN_8O_{0.50}$	$C_{30}H_{35}ClN_8O_{14}$	$C_{54}H_{58}F_6N_{14}O_{19.25}Si$
F_w	1187.11	593.56	699.50	767.11	1353.23
Crystal syst.	triclinic	triclinic	monoclinic	monoclinic	monoclinic
Space group	$P\bar{1}$	$P\bar{1}$	$P21/n$	$P21/n$	$P21/c$
a (Å)	12.8485(8)	8.7155(10)	13.1080(8)	13.0898(10)	13.0590(10)
b Å)	13.7087(8)	11.7684(13)	11.8907(7)	11.7073(9)	10.9712(8)
c (Å)	16.6556(10)	14.0949(16)	21.3416(13)	21.8748(17)	40.322(3)
α (°)	81.6730(10)	88.566(2)	90.00	90.00	90.00
β (°)	78.1930(10)	85.999(2)	93.9650(10)	93.6820(10)	92.696(2)
γ (°)	75.8920(10)	68.624(2)	90.00	90.00	90.00
V (Å^3)	2771.0(3)	1342.9(3)	3318.4(3)	3345.3(4)	5770.6(7)
Z	2	2	4	4	4
D_{calc} (g/cm^3)	1.423	1.468	1.400	1.523	1.558
Crystal size (mm^3)	0.44 × 0.35 × 0.29	0.22 × 0.12 × 0.06	0.48 × 0.44 × 0.36	0.46 × 0.36 × 0.32	0.48 × 0.38 × 0.32
F(0 0 0)	1240	620	1396	1600	2808
μMo K (mm^{-1})	0.109	0.113	1.004	0.198	0.151
T (K)	100(2)	100(2)	100(2)	100(2)	273(2)
θ Range	1.54–28.29	2.36–28.30	1.77–28.28	1.76–28.29	1.56–25.00
Reflections collected	23872	11478	17248	19155	28290
Independent reflections	12545	6056	7052	7712	10153
$R_{(int)}$	0.0241	0.0427	0.0467	0.0306	0.0837
Data/restraints/parameters	12545/0/991	6056/0/480	7052/0/528	7712/0/618	10153/0/888
R_1; wR_2	0.0494; 0.1192	0.0659; 0.1245	0.0467; 0.1375	0.0521; 0.1139	0.0565; 0.1096
GOF (F^2)	1.023	1.000	1.111	1.075	0.941

addition of tetrabutylammonium halide, n-$Bu_4N^+A^-$ salts (where A^- = F^-, Cl^-, Br^- and I^-) to the solution of **L³** in DMSO-d_6, a downfield shift in the N–H resonance is observed in cases of F^-, Cl^- and Br^- (Fig. 1). The downfield shifts of the amide proton ($\Delta\delta$ –N*H*) observed in cases of F^- and Cl^- are 0.1405 and 0.2515 ppm, respectively. There is negligible shift in the N–*H* resonance of **L³** in case of Br^- ($\Delta\delta$ = 0.0356 ppm) whereas no shift is observed with I^-, suggesting non interacting nature of this ion and very weak interaction with Br^- toward **L³**. In cases of oxy-anions such as NO_3^-, ClO_4^-, HSO_4^- no change in chemical shift of the N–*H* resonance of **L³** is observed. This solution study indicates that the binding of I^- as well as any oxy-anion with the **L³** are energetically unfavorable though theoretical investigation suggested that **L³** could be a good receptor for NO_3^- [33]. Instead of NO_3^- binding, **L³** showed binding toward spherical anions like F^-, Cl^-, and Br^- which is clearly evident from the amide N–*H* peak shift of the neutral receptor (Fig. 1).

In case of **L¹** addition of n-$Bu_4N^+F^-$ led to the enormous downfield shift of –N*H* resonance with high $\Delta\delta$ value of 1.894 ppm in DMSO-d_6 (Fig. 2). Addition of n-$Bu_4N^+Cl^-$ to the solution of **L¹** also shows change in the chemical shift of amide –N*H* resonance with $\Delta\delta$ value of 0.2724 ppm whereas no considerable change in chemical shift observed for Br^-/I^- (Fig. 2) or other oxy-anions salts in similar conditions, indicating their non-interactive nature toward this particular receptor having *para* substituted $-NO_2$ functionality. It is important to note that the shift in the N–*H* peak with F^- here is considerably higher than that observed in the case of **L³** whereas this difference is not prominent in case of Cl^-. This result indeed shows a major influence of positional isomers toward the binding of halides in tripodal amide receptors which is strengthen by our further study with the *ortho* isomer i.e. **L²**. Fig. 3 shows the chemical shift change observed by the addition of halides to **L²** in DMSO-d_6 at RT. Interestingly in this case only F^- shows a substantial change in the chemical shift of the amide -N*H* proton. The downfield shift of the amide proton observed with $\Delta\delta$ of 1.052 ppm for this ion where as there is no considerable shift observed for Cl^-, Br^-, and I^- (Fig. 3) or any oxy-anions. This solution ^{1}H NMR study clearly indicates, **L²** as a selective and exclusive receptor for F^- in DMSO.

It is also evident from Figs. 1–3, that concomitant downfield shifts of aromatic hydrogens are observed upon addition of F^- or Cl^- to **L¹** or **L³**, indicating the participation of aromatic –C*H* protons in the halide binding event. It is also noticed that in case of **L¹** upon addition of F^- both the aromatic hydrogen H_a and H_b are shifted (Fig. 2), whereas on addition of Cl^- to the receptor shows downfield shift of only the H_b protons (*meta* to nitro group) which is in close proximity to the amide –N*H* and hence could bind to the Cl^- more effectively. There is no significant change in chemical shift of aromatic protons upon addition of other anions (Br^-, I^-, $H_2PO_4^-$, HSO_4^-, ClO_4^- and NO_3^-). An appreciable change in chemical shift of –C*H* resonances is noticed for **L²** only in case of F^- (as observed in the case of chemical shift of –NH proton) whereas no considerable shift is noticed upon addition of any other anions, further showing the selectivity of **L²** toward F^-. The disturbance in the aromatic –CH protons is also observed in cases of F^-/Cl^-/Br^- binding to **L³**, indicating the participation of –CH protons in the anion binding event. Thus, binding of halides to the respective receptor in solution state is clearly evident from ^{1}H NMR analyses where both N–H···X^- and C–H···X^- interactions are present.

To evaluate the halide binding constants in solution, ^{1}H NMR titration experiments are performed with F^-/Cl^- as their tetrabutylammonium salts in DMSO-d_6 with receptors where ever noticeable change in chemical shift is observed. Fig. 4a and b show the change in chemical shift of –N*H* resonances of **L³** upon addition of aliquots of F^- and Cl^-, respectively. The titration curve gives the best fit for 1:1 binding model for host to guest, in agreement

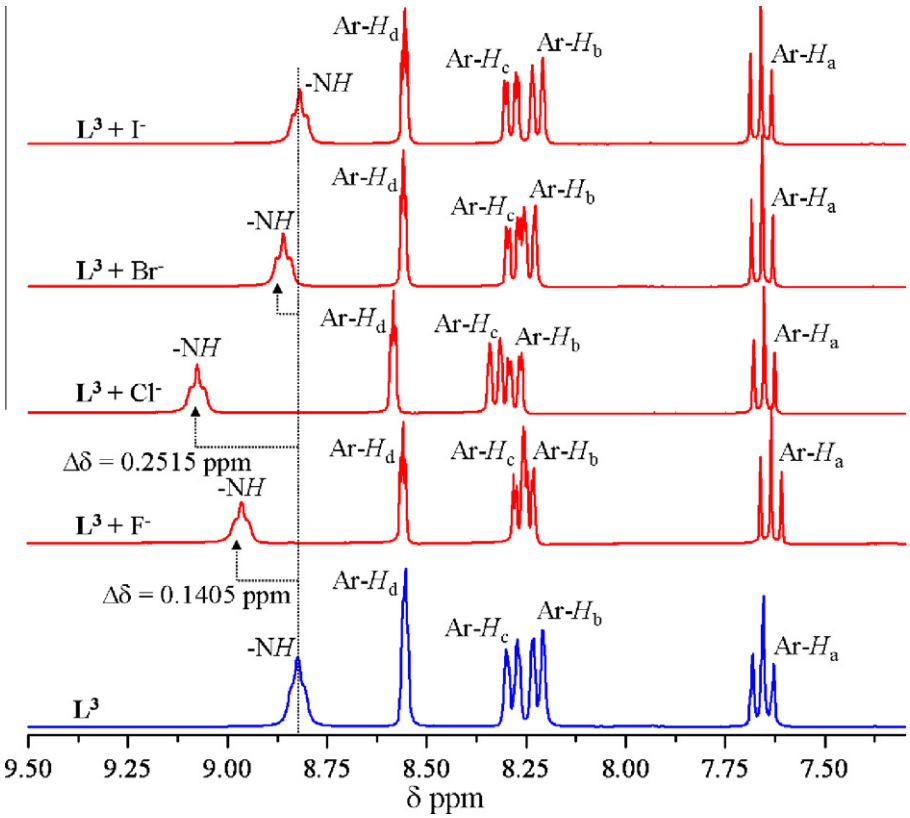

Fig. 1. Partial ^{1}H NMR spectra (300 MHz) of the receptor **L³** in DMSO-d_6 with n-$Bu_4N^+A^-$ (where A^- = F^-, Cl^-, Br^- and I^-) at 298 K.

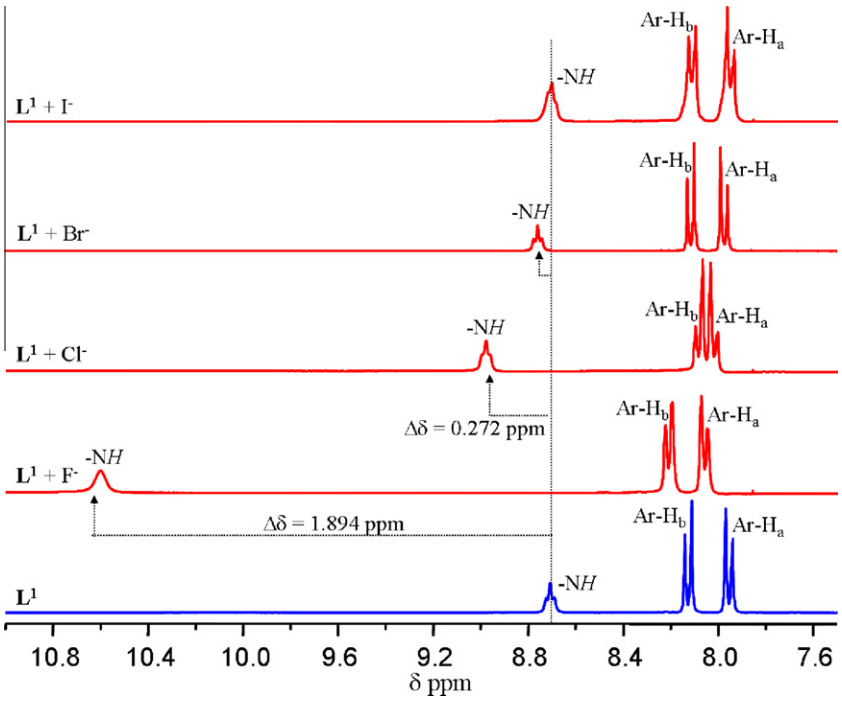

Fig. 2. Partial ^{1}H NMR (300 MHz) spectra of **L^1** in DMSO-d_6 with n-Bu$_4$N$^+$A$^-$ (where A$^-$ = F$^-$, Cl$^-$, Br$^-$ and I$^-$) at 298 K.

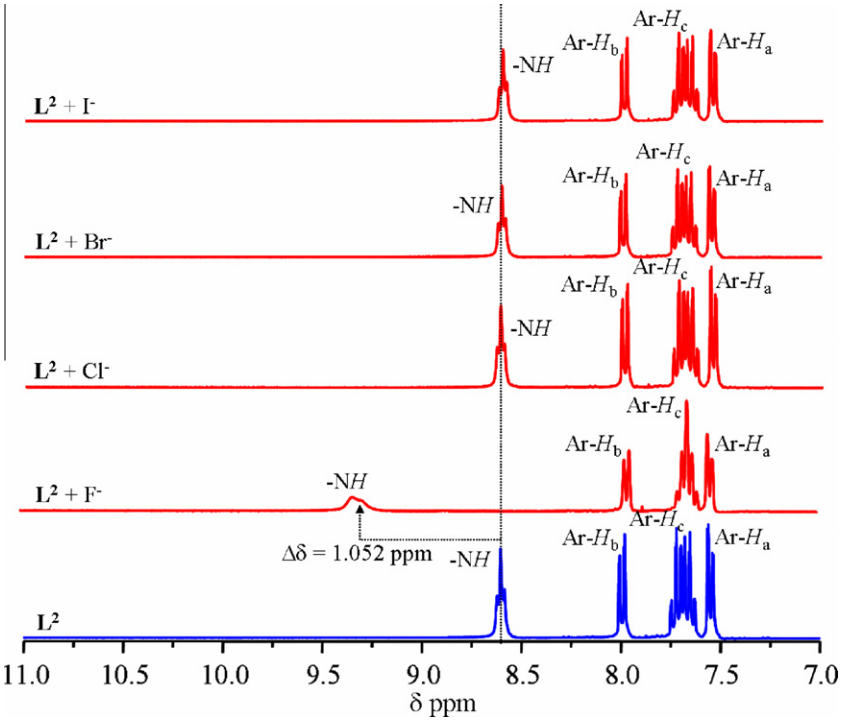

Fig. 3. Partial ^{1}H NMR (300 MHz) spectra of **L^2** in DMSO-d_6 with n-Bu$_4$N$^+$A$^-$ (where A$^-$ = F$^-$, Cl$^-$, Br$^-$ and I$^-$) at 298 K.

with Job's plots indicating a maximum $\Delta\delta$ at 0.5 = [**L^1**]/([**L^1**] + [A$^-$]) and the binding constants are calculated using WINEQNMR 2 [38]. Binding constant data are summarized in Table 2. It is clear from Table 2 that binding constants of **L^3** toward F$^-$ and Cl$^-$ are comparable.

Fig. 5a and b show the solution binding of **L^1** with F$^-$ and Cl$^-$, respectively. The ^{1}H NMR titration curve in these cases also gives the best fit for 1:1 binding model for host to guest. The binding constant data (Table 2) show that **L^1** binds very strongly towards F$^-$ than chloride having log K > 4.0. However Cl$^-$ also displays significant binding but other halides has no binding with **L^1**. Therefore, with the increasing size i.e decreasing basicity of halides the association constant regularly diminishes which is clearly evident in this case.

This receptor **L^2** is showing selective solution state binding with F$^-$ with a large shift of amide –N*H* peak. Fig. 6 shows the titration

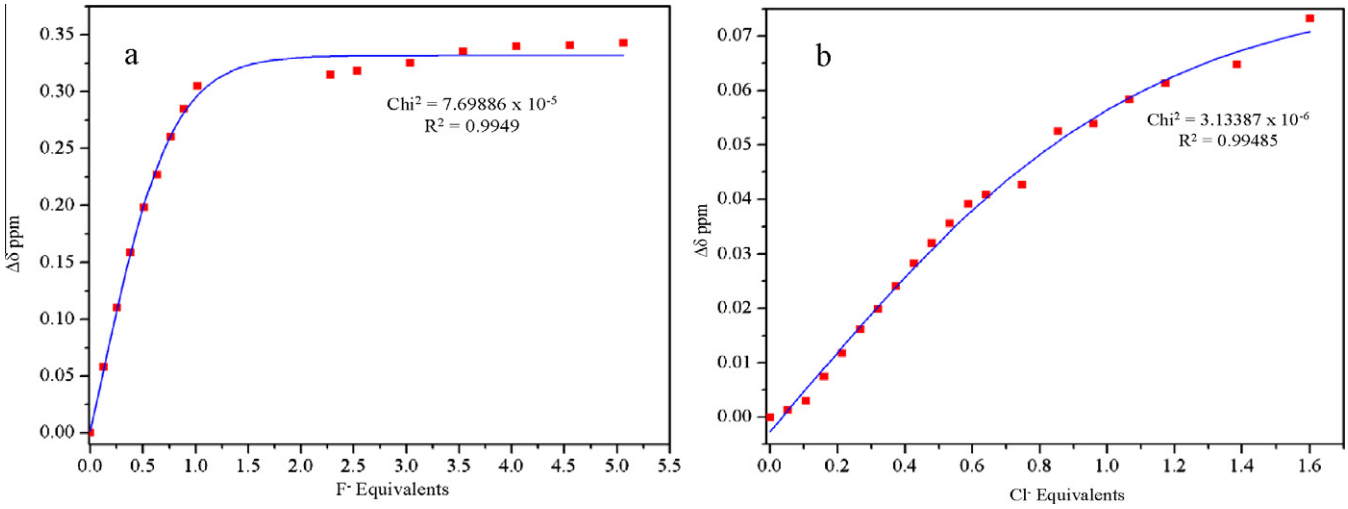

Fig. 4. Change in chemical shift of –NH resonance of $\mathbf{L^3}$ (20 mM) with increasing amounts of (a) n-$Bu_4N^+F^-$ and (b) n-$Bu_4N^+Cl^-$ in DMSO-d_6 at 298 K.

of $\mathbf{L^2}$ with the aliquots of n-$Bu_4N^+F^-$ in DMSO-d_6 at room temperature. Titration data again gives the best fit for a 1:1 association of host to guest as observed in the earlier cases. Binding constant calculated for $\mathbf{L^2}$ with F^- is maximum in this series with the value of log K 5.63 M^{-1} (Table 2).

5. Solid state studies

5.1. Crystallographic studies

5.1.1. L^1

The receptor $\mathbf{L^1}$ crystallizes in triclinic space group $P\bar{1}$ (Table 1), and the ORTEP diagram of the receptor moiety with atom numbering scheme is depicted in Fig. 5S. The same atom numbering for $\mathbf{L^1}$ is retained in all the structures **1–3** presented in this investigation. The single crystal X-ray structure of $\mathbf{L^1}$ shows strong intramolecular and intermolecular hydrogen-bonding interactions between two arms of the tripodal receptor and two other adjacent molecules, respectively.

Table 2
Association constants for $\mathbf{L^1}$–$\mathbf{L^3}$ with different halides in DMSO-d_6 at 298 K.

Receptor	Anions	log K (M^{-1})
L^1	F^-	4.06
	Cl^-	2.29
L^2	F^-	5.63
	Cl^-	–
L^3	F^-	3.76
	Cl^-	3.32

Amide oxygen O1 of one arm acts as an acceptor and is involved in strong intramolecular N–H···O interaction with the donor amide hydrogen H6C (N6–H5C···O1; N6···O1 = 2.946(3) Å, H5C···O1 = 2.18(3) Å, and <N6–H5C···O1 = 150(2)°) (Fig. 7). Further, the receptor is also involved in four strong intermolecular N–H···O and six C–H···O hydrogen-bonding interactions with two adjacent $\mathbf{L^1}$ molecules. Details of these hydrogen-bonding interactions are presented in Table 3.

Solid state crystal structure of the receptor $\mathbf{L^1}$ shows a C_{3v} symmetric cavity which could be suitable for guest encapsulation (N···N distances are 4.284, 4. 290 and 4.484 Å). Of course, the presence of strong intramolecular hydrogen bonding might resists the opening of the tripodal amide receptor cavity. The torsion angles involving $N1_{apical}CCN_{amide}$ are in folded conformation with angles 70.72, 54.97, and 48.81° for three arms composed of the amide nitrogen atoms N2, N4, and N6, respectively, whereas torsion angles involving the carbon atoms connecting the terminal phenyl

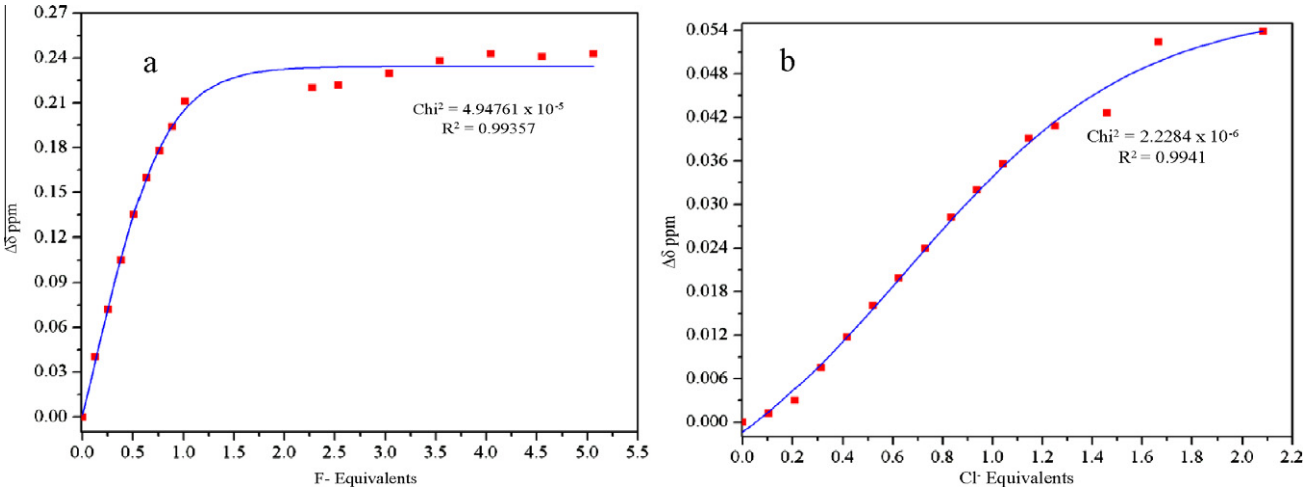

Fig. 5. Change in chemical shift of –NH resonance of $\mathbf{L^1}$ (20 mM) with increasing amounts of (a) n-$Bu_4N^+F^-$ and (b) n-$Bu_4N^+Cl^-$ in DMSO-d_6 at 298 K.

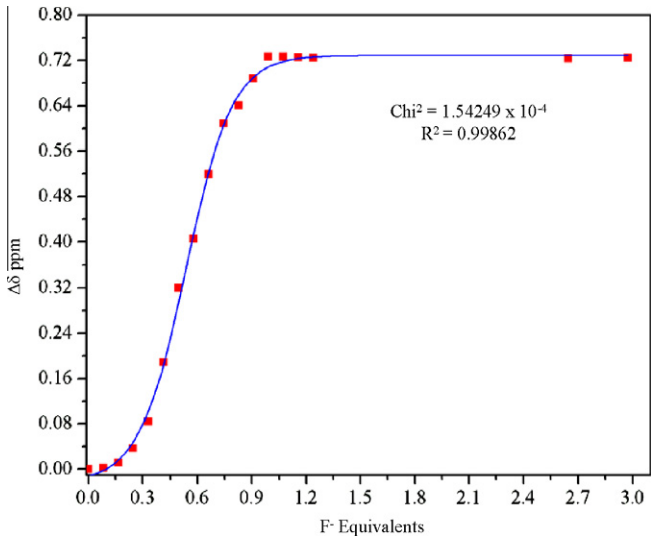

Fig. 6. Change in chemical shift of –NH resonance of $\mathbf{L^2}$ (20 mM) with increasing amounts of n-$Bu_4N^+F^-$ in DMSO-d_6 at 298 K.

rings in each arm are almost in extended conformation with angles 170.10, −175.29, and 179.46°, respectively.

5.2. Crystallographic studies

5.2.1. $\mathbf{L^2}$

The neutral triamide receptor $\mathbf{L^2}$ crystallizes in triclinic space group $P\bar{1}$ (Table 1) with two asymmetric units, and the ORTEP diagram of the receptor moiety with atom numbering scheme is depicted in Fig. 6S. The crystal structure of $\mathbf{L^2}$ also shows strong intramolecular and intermolecular hydrogen-bonding interactions between two arms of the tripodal receptor and other two adjacent molecules, respectively (Fig. 8). Amide oxygen O1 and O16 of two different molecules in the asymmetric unit is involved in strong N–H···O interactions with the donor amide hydrogen atoms H6C (N6–H6C···O1; N6···O1 = 2.8496(18) Å and <N6–H6C···O1 = 150(2)°) and H9C (N9–H9C···O16; N9···O16 = 2.8665(17) Å and <N6–H6C···O1 = 168(2)°), respectively. Further, the receptor is also involved in four strong intermolecular N–H···O hydrogen-bonding interactions with two adjacent $\mathbf{L^2}$ molecules. Details of these hydrogen-bonding interactions are shown in Table 4.

These intramolecular and intermolecular hydrogen bonds resist the formation of C_{3v} symmetric like cavity, which is also evident from the N···N distances of the three arms of the receptor. The torsion angles involving $N1_{apical}CCN_{amide}$ are in folded conformation with angles 73.31, 76.93, and 49.41° for three arms composed of the amide nitrogen N2, N4, and N6, respectively, whereas torsion angles involving the carbon atoms connecting the terminal phenyl rings in each arm are almost in extended conformation with angles −179.15, 179.81, and 176.06°, respectively.

5.2.2. $\mathbf{L^1H^+I^-}$·DMF, **1**

The complex **1** crystallizes in monoclinic space group $P21/n$ (Table 1), and the tertiary nitrogen of the tripodal amide receptor is protonated and turns out to be the mono iodide salt of the $\mathbf{L^1}$ with one molecule of DMF as lattice solvent. The *endo* oriented proton H1C of the apical amine is in N–H···O intramolecular hydrogen bonding with one of the amide oxygen (O7) of the receptor without encapsulation of iodide anion within the C_{3v} cavity of the receptor. It is evident from Fig. 9, that the one iodide anion is surrounded by three protonated $\mathbf{L^1}$ moieties having four hydrogen-bonding contacts (Fig. 9 and Table 5). These are one N–H···I^- interactions of the amide nitrogen atom, N6 and three contacts *via* C–H···I^- interactions from the *meta*, *ortho* hydrogens with respect to the nitro group of the phenyl ring and methlyenic protons of the tren architecture. The tetracoordinated I^- is in distorted square planar geometry. The N···I^- distances is 3.56 Å with N–H···I^- 169.7°, which is in good agreement with the reported values [45,46]. H8 (*ortho*) and H23 (*meta*) with respect to nitro of aryl moiety interact with the I^- with C···I^- distances of 4.034 and 4.018 Å and C–H···I^- angles of 156.1 and 160.8°, respectively, whereas H19A of methylene carbon (C19) interacts with I1 with C···I^- distances of 4.051 Å and C–H···I angle of 156.5°. Thus, the four-point contact *via* N–H···I^- and C–H···I^- interactions is responsible for the binding of the iodide ion with the protonated $\mathbf{L^1}$ receptor outside the tren cavity.

Table 3
Intermolecular hydrogen-bonding interactions of $\mathbf{L^1}$.

D–H···A	d(H···A) Å	d(D···A) Å	<DHA (°)
N2–H2C···O4	2.01(3)	2.911(3)	171(3)
N4–H4C···O7	2.05(3)	2.902(3)	161(3)
C9–H9···O4	2.41(3)	3.21(3)	141(2)
C14–H14···O7	2.38(3)	3.258(3)	156(2)
C18–H18···O4	2.65(2)	3.595(3)	172(2)

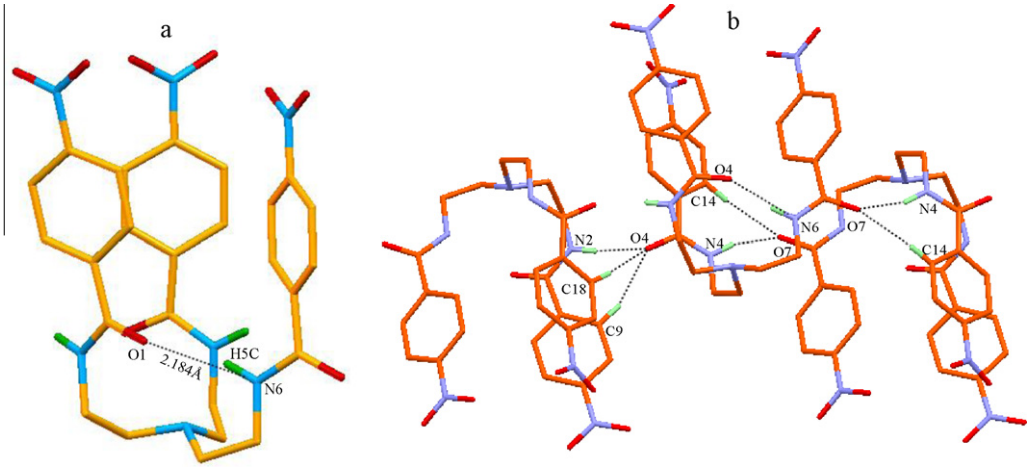

Fig. 7. $\mathbf{L^1}$ showing (a) intramolecular and (b) intermolecular interactions *via* N–H···O and N–H···O hydrogen bonds. Non-acidic hydrogens are omitted for clarity.

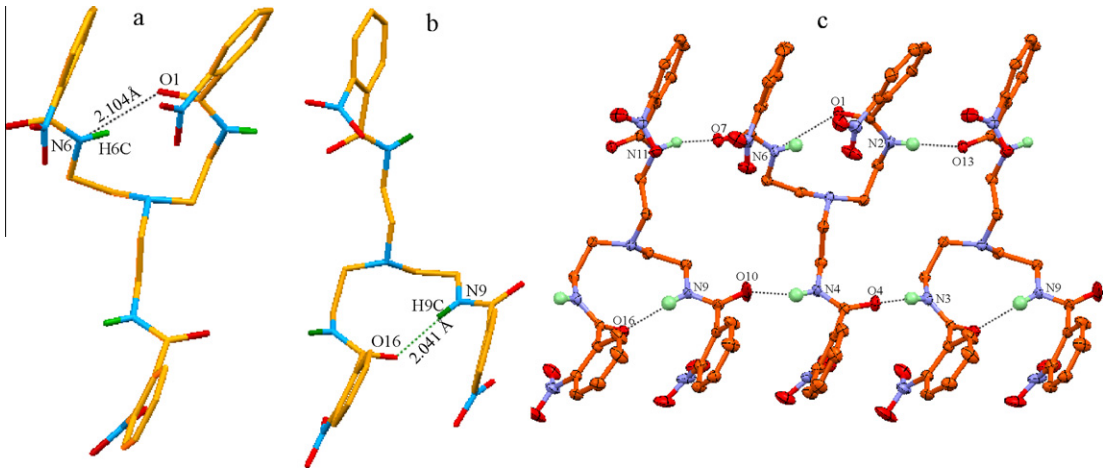

Fig. 8. L^2 showing (a) intramolecular and (b) intermolecular interactions *via* N–H···O hydrogen bonds. Non-acidic hydrogens are omitted for clarity.

Table 4
Intermolecular hydrogen-bonding interactions of L^2.

D–H···A	d(H···A) Å	d(D···A) Å	<DHA (°)
N2–H2C···O13	1.95(2)	2.8252(18)	176(2)
N4–H4C···O10	1.89(2)	2.720(2)	158(2)
N11–H11C···O7	1.92(2)	2.7122(18)	154.8(18)
N13–H13C···O4	2.04(2)	2.8767(19)	172.4(19)

Table 5
Hydrogen-bonding interactions between iodide and surrounding L^1H^+ in complex **1**.

D–H···A	d(H···A) Å	d(D···A) Å	<DHA (°)
N6–H6C···I1	2.96(6)	3.562(4)	170(4)
C8–H8···I1	3.14(8)	4.034(4)	156(2)
C19–H19A···I1	3.15(9)	4.051(4)	157(3)
C23–H23···I1	3.04(5)	4.018(4)	161(3)

The packing diagram of complex **1** (See supporting information, Fig. 10S) viewed down the *b*-axis shows that the cationic array of the receptor is arranged diagonal to the *ac*-plane with chloride between the adjacent bilayers. The receptor moieties are organized *via* intermolecular C–H···O interactions between the alkyl hydrogen from all three arms of the L^1 with oxygen atoms from each nitro group. The lattice DMF molecules interact with receptor molecules *via* strong N–H···O and C–H···O interactions.

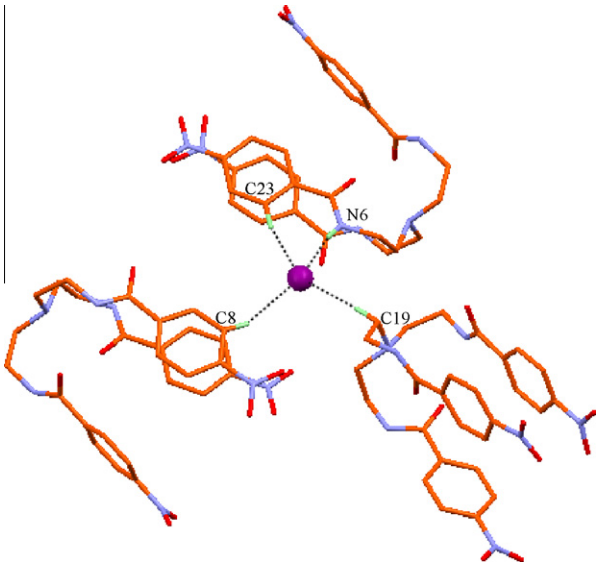

Fig. 9. MERCURY diagram depicting the interactions of the iodide (pink with dotted black hydrogen bonds) with three surrounding L^1H^+ *via* four 4 hydrogen bonds (For interpretation of the references to colour in this figure legend, the reader is referred to the web version of this article.).

5.2.3. $L^2H^+ClO_4^-\cdot DMF$, **2**

Complex **2** crystallizes in a monoclinic *P*21/*n* space group with one molecule of DMF as lattice solvent. In complex **2**, similar intramolecular N–H···O hydrogen bonding exists as observed in **1**. In complex **1**, a similar bilayer arrangement of the receptor moiety is retained *via* various C–H···O and N–H···O interactions as depicted in the packing diagram of **2** (Fig. 11S). Each perchlorate ion is encircled by five monoprotonated L^1 and one lattice DMF molecule having 12 contacts (Fig. 10a and Table 6). A close-up view of perchlorate binding with the receptor is shown in Fig. 10b for clarity. O10 of the perchlorate ion is making two C–H···O (*ortho* hydrogen H17 and methylene proton adjacent to protonated bridgehead nitrogen, H1B) interaction. O11 of perchlorate anion is making four contacts with two receptor units *via* one N–H···O and three C–H···O interactions with amide hydrogen (H6C) and methylenic hydrogens adjacent to the protonated bridgehead nitrogen H10A, H19A and H20B, respectively. O12 is involved in three weak C–H···O contacts with two receptor units (methylenic hydrogen, H11A and H6 of aryl unit, ortho to nitro group) and one lattice DMF molecule (H29B). O13 is in three points with two receptor units via two C–H···O and one N–H···O. Aryl protons H23 (*meta* to nitro group) and H24 (*ortho* to nitro group) are involved in strong C–H···O interactions with O13, whereas O13 is also hydrogen bonded to amide hydrogen (H6C) *via* strong N–H···O interaction. In overall the perchlorate anion is encircled *via* ten C–H···O and two N–H···O contacts.

5.2.4. $L^2H^+0.5\cdot SIF_6^{2-}\cdot H_2O$, **3**

Hexafluorosilicate salt **3** was obtained on reaction of the tripodal receptor L^1 with HF, presumably as a result of glass corrosion. The asymmetric unit of the salt contains two protonated tripodal cations with one SiF_6^{2-} and two water molecules (O19 and O20) as solvent of crystallization. In an attempt to understand the binding of polyatomic anion (SiF_6^{2-}) by the protonated receptor L^1H^+ and lattice water molecule, we have analyzed the interaction of SiF_6^{2-} with the surrounding receptor units (Fig. 11). The fluoride

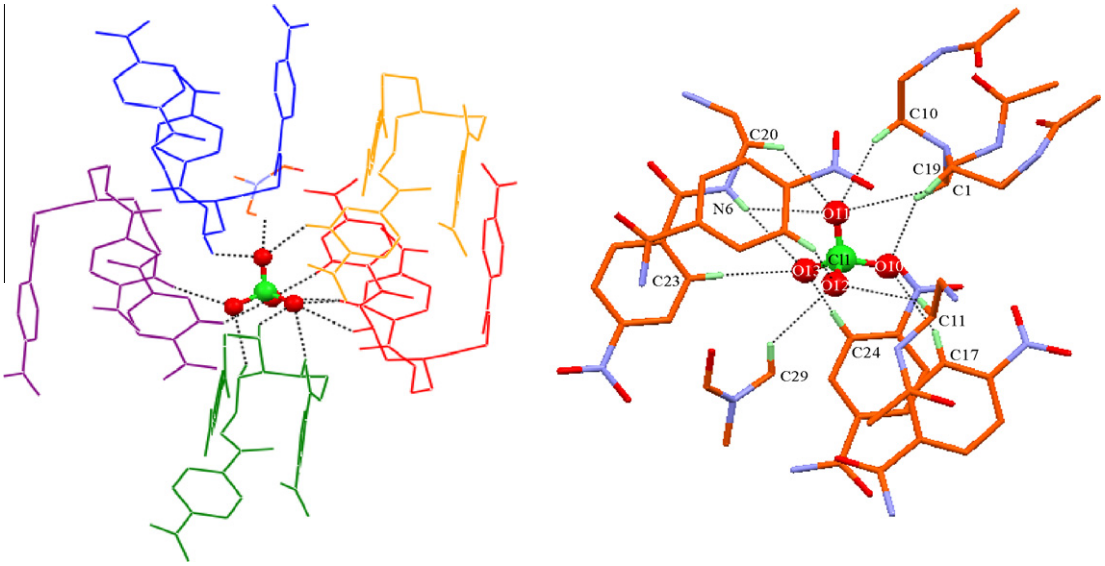

Fig. 10. MERCURY diagram depicting (a) the interactions of the perchlorate anion with five surrounding $\mathbf{L^1}H^+$ units and one lattice DMF molecule *via* C–H···O and N–H···O hydrogen bonds. (b) Close-up view of perchlorate anion binding. Non-acidic hydrogens are omitted for clarity.

Table 6
Hydrogen-bonding interactions between perchlorate anion and surrounding $\mathbf{L^1}H^+$ in complex **1**.

D–H···A	d(H···A) Å	d(D···A) Å	<DHA (°)
C1–H1B···O10	2.60(2)	3.317(3)	134(3)
C17–H17···O10	2.41(2)	3.320(3)	160.4(18)
C20–H20B···O11	2.57(2)	3.313(3)	133.9(19)
C10–H10A···O11	2.64(2)	3.567(3)	160.8(17)
C19–H19A···O11	2.66(2)	3.501(3)	147.2(17)
N6–H6C···O11	2.60(2)	3.199(3)	131.2(17)
C6–H6···O12	2.59(2)	3.109(3)	114.3(17)
C11–H11A···O12	2.52(2)	3.232(3)	128.4(17)
C29–H29B···O12	2.59(2)	3.231(3)	126.2(19)
C23–H23···O13	2.41(2)	3.320(3)	170.2(19)
C24–H24···O13	2.50(2)	3.306(3)	142.8(19)
N6–H6C···O13	2.59(3)	3.385(3)	165(2)

atoms (F1, F2, F3 and F5) of SiF_6^{2-} are each making three contacts, whereas F4 and F6 is making four and two contacts, respectively with the surrounding receptor moieties and lattice water resulting in 18 hydrogen-bonding contacts on SiF_6^{2-}. F1 and F2 is involved in the two N–H···F and one C–H···F interactions each with receptor units. F3 is involved in three weak C–H···F contact with the methylene hydrogens, whereas F4 is in bonding *via* three C–H···F (alkyl hydrogens H28B, H37A and H37B) and one O–H···F (lattice water hydrogen H19C) (Table 7). F5 is in three point contact with surrounding receptor units via two C–H···F (methylene hydrogens H46A and H47B) and one N–H···F (amide hydrogen H6C) interactions. The F6 of SIF_6^{2-} is weakly hydrogen bonded to one aryl C–H and one O–H of the receptor and lattice water molecules, respectively. The observed C–H···F and N–H···F interaction distance and angles are within the range reported in the literature [45].

6. Conclusion

The solution-state ^{1}H NMR study of anion binding with tripodal triamide receptors, $\mathbf{L^1}$–$\mathbf{L^3}$ shows that positional isomers have an important role toward the selectivity. All three neutral receptors bind selectively with halides whereas no solution-state binding is

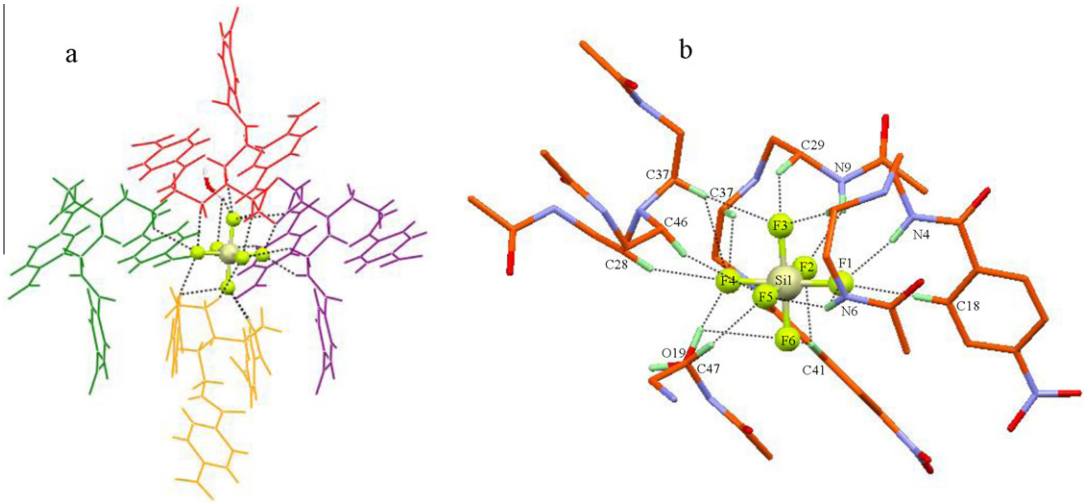

Fig. 11. MERCURY diagram depicting (a) the interactions of the hexafluorosilicate anion with four surrounding $\mathbf{L^1}H^+$ units and one lattice water molecule *via* C–H···F, N–H···F and O–H···F hydrogen bonds. (b) Close-up view of SiF_6^{2-} anion binding. Non-acidic hydrogens are omitted for clarity.

Table 7
Hydrogen-bonding interactions between hexafluorosilicate anion and surrounding $\mathbf{L^1}H^+$ in complex **3**.

D–H···A	d(H···A) Å	d(D···A) Å	<DHA (°)
N4–H4C···F1	1.926	2.796(4)	167.1
N6–H6C···F1	2.460	2.833(4)	111.4
C18–H18···F1	2.401	3.226(4)	147.8
N9–H9C···F2	2.071	2.796(5)	145.4
N11–H11C···F2	1.922	2.733(5)	156.9
C41–H41···F2	2.447	3.221(4)	140.6
C19–H19A···F3	2.479	3.389(5)	156.4
C29–H29B···F3	2.353	3.172(4)	141.8
C37–H37A···F3	2.395	3.332(4)	162.2
C28–H28B···F4	2.245	3.129(5)	151.2
C37–H37A···F4	2.584	3.325(4)	133.2
C37–H37B···F4	2.638	3.420(5)	137.8
O19–H19C···F4	1.707	2.735(4)	158.0
N6–H6C···F5	2.225	2.897(4)	146.1
C46–H46A···F5	2.612	3.520(5)	155.6
C47–H47B···F5	2.420	3.022(5)	119.8
C41–H41···F6	2.343	3.211(4)	155.1
O19–H19C···F6	2.589	3.060(4)	165.6

observed in cases of any oxyanions. Among three receptors *ortho* isomer, $\mathbf{L^2}$ shows exclusive binding toward only fluoride in the halide series. Though $\mathbf{L^1}$ shows binding toward fluoride as well as chloride but it acts as a fluoride selective receptor as evident from binding constant data. On the other hand $\mathbf{L^3}$ does not show selectivity among fluoride and chloride in solution-state study. Solution-state binding of halides in the above cases indicate the participation of amide –NH and aryl-CH protons in anion binding process. The solid-state structural study of *para*-isomer, $\mathbf{L^1}$ shows that two of the three amide functional groups present in the ligand are in strong intramolecular hydrogen-bonding interactions which create a C_{3v} symmetric cleft which could be suitable for encapsulation of anionic guest. On the other hand *ortho*-isomer, $\mathbf{L^2}$ has two different conformations in an asymmetric unit where each of the unit is involved one intramolecular hydrogen-bonding interactions between two amide groups. This receptor does not possess symmetric cleft could be due to the bulky nitro substitution at the *ortho* position. Structural studies of the anion binding with the protonated triamide receptor $(H\mathbf{L^1})^+$ shows that not one of the guests is encapsulated inside the tren arm irrespective of size, shape, and charge of the anions. However, detailed structural investigation clearly demonstrates that the self-alignment, preorganization, and orientation of the multiple ligand moieties, depending upon the dimensionality of the incoming anionic guest, play a crucial role in making various molecular interactions in the binding of the anion outside the tripodal cavity. In all the complexes of $(H\mathbf{L^1})^+$, (**1**–**3**), amide N–H and aryl C–H···anion hydrogen bonds form mostly by the *meta* hydrogen with respect to the $-NO_2$ group and in some cases with the *para* hydrogen.

Acknowledgements

P.G. Gratefully acknowledges the Council for Scientific and Industrial Research (CSIR), New Delhi, India (Grant No. 01(2225)/08/EMR-II) for financial support. X-ray Crystallography study is performed at the DST-funded National Single Crystal X-ray Diffraction Facility at the Department of Inorganic Chemistry, IACS.

Appendix A. Supplementary material

^{1}H NMR, and HRMS of $\mathbf{L^1}$ and $\mathbf{L^2}$. ORTEP diagrams of $\mathbf{L^1}$, $\mathbf{L^2}$ and complexes **1**–**3**; packing diagrams of complexes **1** and **2**. CCDC 760005, 760006, 760007, 760008 and 760009 contain the supplementary crystallographic data for this paper. These data can be obtained free of charge from The Cambridge Crystallographic Data Centre via www.ccdc.cam.ac.uk/data_request/cif. Supplementary data associated with this article can be found, in the online version, at doi:10.1016/j.ica.2010.02.030.

References

[1] A. Bianchi, K. Bowman-James, E. García-España (Eds.), Supramolecular Chemistry of Anions, Wiley-VCH, New York, 1997.
[2] P.D. Beer, P.A. Gale, Angew. Chem., Int. Ed. 40 (2001) 486.
[3] J.M. Llinares, D. Powell, K. Bowman-James, Coord. Chem. Rev. 240 (2003) 57.
[4] J.L. Atwood, J.W. Steed (Eds.), The Encyclopedia of Supramolecular Chemistry, Dekker, New York, 2004.
[5] K. Bowman-James, Acc. Chem. Res. 38 (2005) 671.
[6] E. García-España, P. Díaz, J.M. Llinares, A. Bianchi, Coord. Chem. Rev. 250 (2006) 2952.
[7] K. Wichmann, B. Antonioli, T. Söhnel, M. Wenzel, K. Gloe, K. Gloe, J.R. Price, L.F. Lindoy, A.J. Blake, A. Schröder, Coord. Chem. Rev. 250 (2006) 2987.
[8] B.L. Schottel, H.T. Chifotides, K.R. Dunbar, Chem. Soc. Rev. 37 (2008) 68.
[9] A. Bianchi, K. Bowman-James, E. García-España (Eds.), Supramolecular Chemistry of Anions, Wiley-VCH, New York, 1997.
[10] S.S. Zhu, H. Staats, K. Brandhorst, J. Grunenberg, F. Gruppi, E. Dalcanale, A. Lützen, K. Rissanen, C.A. Schalley, Angew. Chem., Int. Ed. 47 (2008) 788.
[11] M. Albrecht, C. Wessel, M. de Groot, K. Rissanen, A. Lüchow, J. Am. Chem. Soc. 130 (2008) 4600.
[12] Y. Li, A.H. Flood, Angew. Chem., Int. Ed. 47 (2008) 2649.
[13] R.J. Götz, A. Robertazzi, I. Mutikainen, U. Turpeinen, P. Gamez, J. Reedijk, Chem. Commun. (2008) 3384.
[14] C. Caltagirone, P.A. Gale, J.R. Hiscock, S.J. Brooks, M.B. Hursthouse, M.E. Light, Chem. Commun. (2008) 3007.
[15] R.B. Bedford, M. Betham, C.P. Butts, S.J. Coles, M.B. Hursthouse, P.N. Scully, J.H.R. Tucker, J. Wilkie, Y. Willener, Chem. Commun. (2008) 2429.
[16] D.R. Turner, M.J. Paterson, J.W. Steed, Chem. Commun. (2008) 1395.
[17] K.-Y. Ng, V. Felix, S.M. Santos, N.H. Rees, P.D. Beer, Chem. Commun. (2008) 1281.
[18] C. Caltagirone, G.W. Bates, P.A. Gale, M.E. Light, Chem. Commun. (2008) 61.
[19] C. Schmuck, V. Bickert, J. Org. Chem. 72 (2007) 6832.
[20] O.B. Berryman, A.C. Sather, B.P. Hay, J.S. Meisner, D.W. Johnson, J. Am. Chem. Soc. 130 (2008) 10895.
[21] S. Valiyaveettil, J.F.J. Engbersen, W. Verboom, D.N. Reinhoudt, Angew. Chem., Int. Ed. Engl. 32 (1993) 900.
[22] P.D. Beer, Z. Chen, A.J. Goulden, A. Graydon, S.E. Stokes, T. Wear, J. Chem. Soc. Chem. Commun. (1993) 1834.
[23] P.D. Beer, P.K. Hopkins, J.D. McKinney, Chem. Commun. (1999) 1253.
[24] C. Raposo, M. Almaraz, M. Martín, V. Weinrich, Mª.L. Mussóns, V. Alcázar, Mª.C. Caballero, J.R. Morán, Chem. Lett. (1995) 759.
[25] A. Danby, L. Seib, K. Bowman-James, N.W. Alcock, Chem. Commun. (2000) 973.
[26] C. Bazzicalupi, A. Bencini, E. Berni, A. Bianchi, S. Ciattini, C. Giorgi, S. Maoggi, P. Paoletti, B. Valtancoli, J. Org. Chem. 67 (2002) 9107.
[27] K. Kavallieratos, A. Danby, G.J. Van Berkel, M.A. Kelly, R.A. Sachleben, B.A. Moyer, K. Bowman-James, Anal. Chem. 72 (2000) 5258.
[28] P.S. Lakshminarayanan, E. Suresh, P. Ghosh, Inorg. Chem. 45 (2006) 4372.
[29] R. Custelcean, B.A. Moyer, B.P. Hay, Chem. Commun. (2005) 5971.
[30] D.A. Jose, D.K. Kumar, B. Ganguly, A. Das, Inorg. Chem. 46 (2007) 5817.
[31] R. Custelcean, P. Remy, P.V. Bonnesen, De-en. Jiang, B.A. Moyer, Angew. Chem., Int. Ed. 47 (2008) 1866.
[32] B. Wu, J. Liang, J. Yang, C. Jia, X.-J. Yang, H. Zhang, N. Tang, C. Janiak, Chem. Commun. (2008) 1762.
[33] V.S. Bryantsev, B.P. Hay, Org. Lett. 7 (2005) 5031.
[34] M.A. Hossain, J.A. Liljegren, D. Powell, K. Bowman-James, Inorg. Chem. 43 (2004) 3751.
[35] P.S. Lakshminarayanan, I. Ravikumar, E. Suresh, P. Ghosh, Inorg. Chem. 46 (2007) 4769.
[36] P.S. Lakshminarayanan, I. Ravikumar, E. Suresh, P. Ghosh, Chem. Commun. (2007) 5214.
[37] I. Ravikumar, P.S. Lakshminarayanan, M. Arunachalam, E. Suresh, P. Ghosh, Dalton Trans. (2009) 4160.
[38] M.J. Hynes, J. Chem. Soc., Dalton Trans. (1993) 311.
[39] G.M. Sheldrick, SAINT and XPREP, Version 5.1, Siemens Industrial Automation Inc., Madison, WI, 1995.
[40] SADABS, Empirical Absorption Correction Program, University of Göttingen: Göttingen, Germany, 1997.
[41] G.M. Sheldrick, SHELXTL Reference Manual, Version 5.1, Bruker AXS, Madison, WI, 1997.
[42] G.M. Sheldrick, SHELXL-97, Program for Crystal Structure Refinement, University of Göttingen, Göttingen, Germany, 1997.
[43] A.L. Spek, PLATON-97, University of Utrecht, Utrecht, The Netherlands, 1997.
[44] MERCURY 2.3 Supplied with Cambridge Structural Database, CCDC, Cambridge, UK, 2010.
[45] C.A. Ilioudis, D.A. Tocher, J.W. Steed, J. Am. Chem. Soc. 126 (2004) 12395.
[46] S.O. Kang, J.M. Llinares, D. Powell, D. VanderVelde, K. Bowman-James, J. Am. Chem. Soc. 125 (2003) 10152.